

# Design of frequency reconfigurable antenna for cognitive radio applications

T. R. MUTHU<sup>a</sup>, A. THENMOZHI<sup>b</sup>

<sup>a</sup>*Department of Electronics and Communication Engineering, K.L.N College of Engineering, Sivagangai, Tamil Nadu, India*

<sup>b</sup>*Department of Electronics and Communication Engineering, Kalasalingam University, Tamil Nadu, India*

---

In the recent times, with the explosion of wireless technologies and demand for spectrum efficiency led to the analysis of frequency reconfigurable antenna. This is the next frontier in science and technology for cognitive radio. A frequency reconfigurable antenna with slots in the partial ground plane is proposed. UWB antenna along with reconfigurable features was modeled numerically and self consistently solved with equations. The dimensions of the proposed antenna were designed with the help of the equations. This led to the miniaturization of the antenna and enhancement in bandwidth. The simulated results show that the proposed antennas maintain impedance bandwidth from 3.1 to 11 GHz with simultaneous tunable frequencies. The maximum gain of the antenna is 6.5dB and VSWR is less than 2 over the operating band. The results show that the H plane radiation pattern is omnidirectional over the operating band. The fabricated prototype of frequency reconfigurable antenna with pin diode is done. The measured results shows good agreement with the simulation results for wideband and switching characteristics.

(Received May 21, 2020; accepted June 11, 2021)

*Keyword:* Frequency reconfigurable antennas, Partial ground plane omnidirectional, UWB, Microstrip discontinuity

---

## 1. Introduction

The reconfigurable antenna is an alternative design to single patch antenna, as it can offer controllable radiating properties such as resonance for cognitive radio and wireless communication systems. This property of controlling the mechanism could allow for future-proofing of a system to the changing standards or tuning in the field to match a sensitive wireless environment. The reconfigurability of the reconfigurable antennas is not limited to a single characteristic, but, can be an encapsulation of multiple characteristics relying upon the applications. The frequency reconfigurable antennas play a vital role in any communication system, because they are capable to reconfigure the frequency, radiation pattern and polarization as per the system requirements.

Spread spectrum signals are characterized by their relatively large bandwidth. The requirement is the use of an antenna with the capability of operating within such bandwidths. Spread spectrum signal are most applicable in wireless local area networks (WLAN) and worldwide interoperability for microwave access (WiMAX). Reconfigurable antennas are dynamic antennas which can modify their properties such as radiation pattern, polarization and frequency with changing system requirements or environmental conditions in a controlled and reversible manner. In particular, frequency reconfigurability in antennas is beneficial for diverse applications, as it reduces the bandwidth requirement of spread spectrum signals. This is due to the fact that wireless applications will not need to cover all operating frequencies simultaneously, which in effect will

ameliorate any restriction on antennas and improve their functionalities without increasing their size and complexity. The important characteristics of frequency reconfigurable antennas include their miniaturized size, low cost and use for a variety of applications resulting in their integration into most modern wireless systems.

## 2. Literature review

Earlier, the frequency tuning was generally being achieved by using a Varactor diode thereby redirecting surface currents has been reported [1]. Frequency reconfigurable antennas have pulled a significant attention of the researchers due to their vast applications in communication, electronic surveillance and counter measure [2]. It is predicted that Cognitive Radio (CR) can adapt the way in which spectrum is being allocated [3]. The antennas which are capable to operate on multiband will be the need of future cognitive radio communication systems. The frequency reconfigurable multiband antennas are in high demand for current wireless applications, as they are capable to operate on multiple frequencies. However, fixed multiband antennas usually require complicated filters to avoid interference issues [4]. The use of filters to avoid frequency interference usually adds complexity to any radiation system. The issue of interference can be avoided by frequency reconfigurable antenna. This work aims at an approach to design a frequency reconfigurable antenna using RF switches. The step tapered radiating patch is modeled by numerical calculations. The bandwidth enhancement is obtained due

to step tapered patch antenna and stub insertion. With the help of partial ground plane multiple resonances are obtained. The reconfigurability of the proposed antenna has been achieved by the introduction of slots in the ground plane and changing the states of the RF switches.

### 3. Antenna structure and design

#### 3.1. UWB antenna design

The planar monopole antenna was firstly reported in 1976 by G. Dubost and S. Zisler [5]. UWB planar monopoles developed from conventional UWB antenna has wider bandwidth performance. Planar monopoles are used in antennas due to its volume miniaturization. For portable wireless devices printed planar monopoles are used because of its easy integration [6]. The patch and partial ground plane forms a printed monopole antenna. Both of them are printed on the same or opposite side of a substrate, and a microstrip feedline is used to excite the monopole patch. The proposed geometry used in this work is stub inserted step rectangular printed monopole with partial ground plane which has an impedance bandwidth of 3.8:1 as shown in Fig. 1.

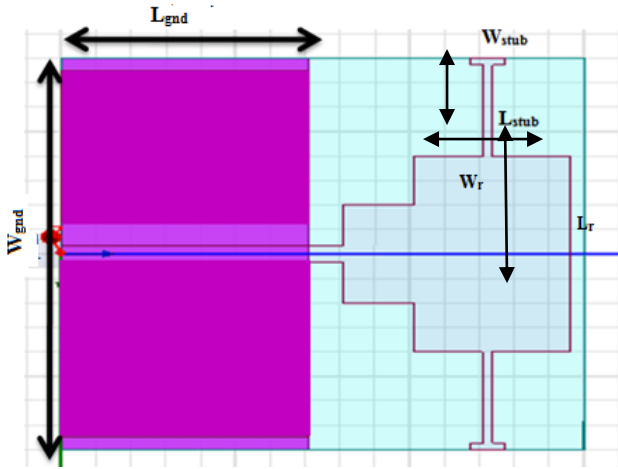


Fig. 1. Structure of proposed UWB antenna (color online)

The proposed design gradually evolved from a square patch radiator, notches at the bottom of the radiator, stub near to the patch for bandwidth enhancement. The partial ground plane in addition to producing resonance, maintains flat impedance bandwidth over the entire operating band.

The transmission line model [7] is used to model the radiator from which the parameters can be obtained. The basic steps in the designing of microstrip patch are selection of resonant frequency and dielectric medium. The width of the patch is calculated using Eq. (1)

$$W = \frac{C_o}{2f_r} \sqrt{\frac{2}{\epsilon_r + 1}} \quad (1)$$

where  $C_o$ =Velocity of light,  $\epsilon_r$ =dielectric constant of the substrate

The radiation from radiator to ground passes through substrate and air medium. The air and the substrate have different dielectric values, so an effective dielectric is discussed in Eq. (2)

Where  $h$  is the height of the substrate

$$\epsilon_{\text{reff}} = \left(\frac{\epsilon_r + 1}{2}\right) + \left(\frac{\epsilon_r - 1}{2}\right) \left[1 + 12 \frac{h}{W}\right]^{-2} \quad (2)$$

where  $h$  is the height of the substrate

If  $W/h \gg 1$  and  $\epsilon_r \gg 1$  then the field were concentrated in substrate. This ratio plays a vital role to identify the effective dielectric constant  $\epsilon_{\text{reff}} < \epsilon_r$ . Due to fringing effects the length of the patch gets expanded and the effective length is calculated using Eq. (3)

$$L_{\text{eff}} = L + 2\Delta L \quad (3)$$

The length and incremental length is carried out in Eqs.(4) and (5)

$$L = \frac{C_o}{2f_r \sqrt{\epsilon_{\text{reff}}}} - 2\Delta L \quad (4)$$

$$\Delta L = 0.412h \left[ \frac{(\epsilon_{\text{reff}} + 0.3) \left(\frac{W}{h} + 0.264\right)}{(\epsilon_{\text{reff}} - 0.258) \left(\frac{W}{h} + 0.8\right)} \right] \quad (5)$$

The length ( $L_g$ ) and width ( $W_g$ ) are the length and width of the ground plane which can be determined using Eqs. (6) and (7)

$$L_g = 6h + L \quad (6)$$

$$W_g = 6h + W \quad (7)$$

The bandwidth can be increased using this transmission line model by increasing the substrate height. With increase in height, the surface wave increases and spreads in and around of the substrate and also in the curves of the patch. This deteriorates the antenna performance. So air gap techniques is used in which surface wave does not come into existence. The fundamental resonant frequency of a printed antenna with a rectangular ground plane can be approximated by using Eq. (8) as given in [8].

$$f_r = \frac{144}{L_g + L_r + g + \frac{A_g}{2\pi L_g \sqrt{\epsilon_e}} + \frac{A_r}{2\pi L_r \sqrt{\epsilon_e}}} \quad (8)$$

Here,  $L_g$  and  $L_r$  are the lengths of ground plane and radiator respectively and  $g$  is the gap between them,  $A_g$

and  $A_r$  are the areas of ground plane and radiator respectively and the effective dielectric constant is predicted as  $\epsilon_e = (\epsilon_r + 1)/2$ , where  $\epsilon_r$  is the dielectric constant of the substrate. In the proposed antenna designs, the cost-effective substrate FR4 (relative permittivity,  $\epsilon_r = 4.4$ , loss tangent,  $\tan\delta = 0.02$ , thickness = 1.6 mm) is used. The evolution of antenna 1 is shown in Fig. 2.

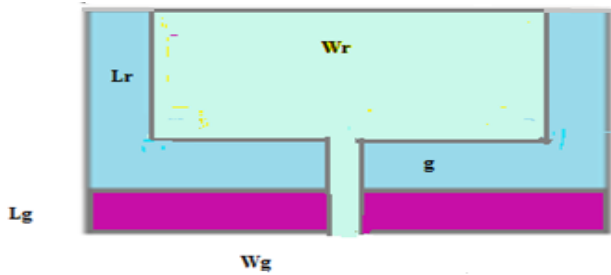


Fig. 2. Evolution of antenna 1-UWB antenna (color online)

The length of the radiator must be  $\lambda_e/4$  at the desired frequency. The length of the ground plane must be at least  $\lambda_e/4$  to obtain wider bandwidth. With these assumptions antenna 1 is designed to estimate its fundamental resonance or lowest resonance. The lowest resonance obtained is 3.9 GHz. The antenna is fed by 50Ω microstrip and the partial ground plane is printed on back side of the substrate. The design parameters for the antenna in Fig. 2 is as follows  $L_r=13$  mm,  $W_r=16$  mm,  $g=2$  mm,  $W_g=32$  mm,  $L_g=14.2$  mm. The simulated results of antenna 1 are shown in Fig. 3.

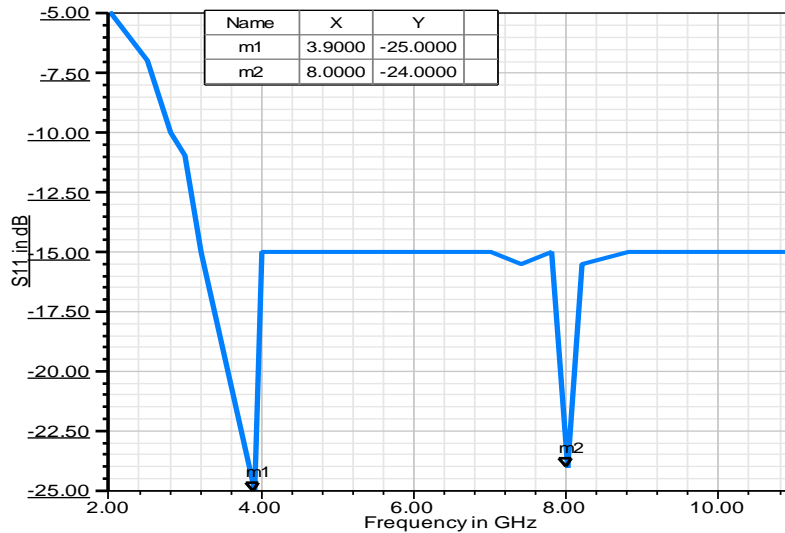


Fig. 3. Simulated results of proposed antenna 1 (color online)

The antenna displays resonant frequencies at 3.9 GHz with return loss of -25 dB and 8 GHz with loss of -24 dB. The lowest resonance is due to the length of the radiator. The second resonance is observed at 8 GHz due to partial ground plane.

The evolution of antenna 2 shown in Fig. 4 leads to the enhancement of bandwidth. The antenna is tapered at the bottom of the patch known as step rectangular patch antenna. This microstrip discontinuity is modeled to find its dimensions since this plays a vital role in improving the bandwidth. This contributes to lowering of peaks and shifting the second resonance to extreme right thereby improving its impedance bandwidth. This is due to the fact the microstrip discontinuity is positioned near the partial ground plane and there exists capacitive coupling between them.

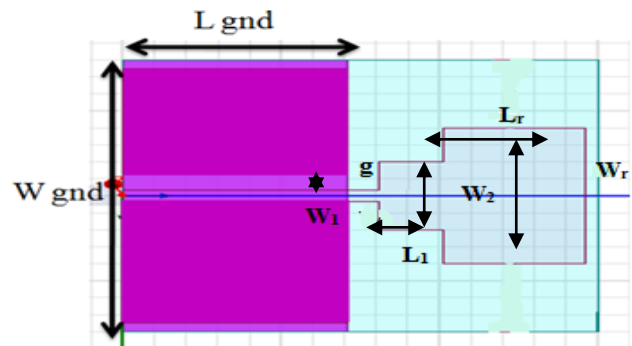


Fig. 4. Evolution of antenna 2- Step rectangular UWB antenna (color online)

At the bottom of the patch there is rapid change in geometry due to tapering at the ends [9]. As can be seen capacitive coupling is formed between patch and ground plane [10]. As the geometry at the ends shifts up and down the spreading of electric and magnetic field is altered. The steps at the edges can be considered as split LC combination as shown in Fig. 5. The Quasi static computation equations can be used to calculate the variables. From these computations the dimensions of  $L_1$  and  $W_1$  can be deduced as follows in Eqs. (9) to (19).

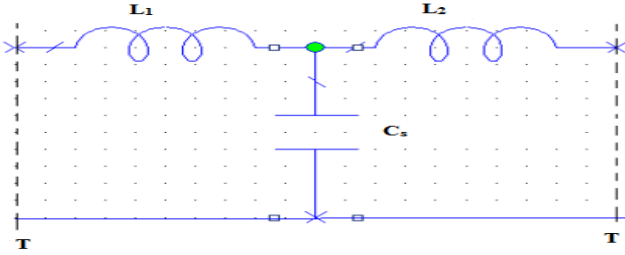


Fig. 5. Microstrip discontinuity circuit (color online)

$$C_s = 0.00137 \frac{\sqrt{\epsilon_{re1}}}{Z_{o1}} \left(1 - \frac{W_1}{W_r}\right) h \frac{(\epsilon_{re1} + 0.3)}{(\epsilon_{re1} - 0.258)} \times \frac{\left(\frac{W_r}{h} + 0.264\right)}{\left(\frac{W_r}{h} + 0.8\right)} \quad (9)$$

$$L_1 = \frac{L_{w1}}{L_{w1} + L_{w2}} L_s \quad (10)$$

$$L_2 = \frac{L_{w2}}{L_{w1} + L_{w2}} L_s \quad (11)$$

$$L_{wi} = \left(\frac{Z_{o1} \sqrt{\epsilon_{reff}}}{c}\right) \quad (12)$$

$$L_s = 0.000987h \left(1 - \frac{Z_{o1}}{Z_{o2}} \sqrt{\frac{\epsilon_{re1}}{\epsilon_{re2}}}\right)^2 \quad (13)$$

where  $c$  is the velocity of light,  $W_r$  is the width of the radiator and  $W_1$  is the width of the feed line  
 $W_2$  is the width of microstrip discontinuity  
 $L_1$  is the change in step length of microstrip discontinuity  
 $C_s$  in picofarads and  $L_s$  in nanoHenry  
 $Z_{o1}$  and  $Z_{o2}$  are the characteristic impedance at port 1 and 2

$$\epsilon_{re1} = \left(\frac{\epsilon_r + 1}{2}\right) + \left(\frac{\epsilon_r - 1}{2}\right) \left[1 + 12 \frac{h}{W_r}\right] \quad (14)$$

$$\epsilon_{re1} = \left(\frac{\epsilon_r + 1}{2}\right) + \left(\frac{\epsilon_r - 1}{2}\right) \left[1 + 12 \frac{h}{W_1}\right] \quad (15)$$

The method of compensating for excess capacitance in a step width change is similar to that used to compensate for that in an open ended line, and is based on an expression (9) for the length correction,  $L_1$ , required

for the lower impedance line,  $W_2$ , proposed by Edwards [11] as follows.

$$\frac{L_1}{h} = 0.412 \frac{\epsilon_{eff} + 0.3}{\epsilon_{eff} + 0.258} = \frac{\frac{W_r}{h} + 0.262}{\frac{W_r}{h} + 0.813} \left[1 - \frac{W_1}{W_2}\right] \quad (16)$$

where  $W_r/h$  is calculated from Eq. (17) as

$$\frac{W_r}{h} = \left[\frac{e^H}{8} - \frac{1}{4e^H}\right]^{-1} \quad (17)$$

The parameter  $H$  is obtained from equation 18

$$H = \frac{Z_o \sqrt{2(\epsilon_r + 1)}}{119.9} + \frac{1}{2} \left(\frac{\epsilon_r - 1}{\epsilon_r + 1}\right) \left[\ln\left(\frac{\pi}{2}\right) + \frac{1}{\epsilon_r} \ln\left(\frac{\pi}{4}\right)\right] \quad (18)$$

Here  $W_r/h > 1$  and hence  $Z_o$  is calculated as follows from Eq. (19)

$$Z_o = \frac{\pi}{\sqrt{\epsilon_{reff}}} \times \frac{120}{\frac{W_r}{h} + 1.393 + 0.667 \ln\left(\frac{W_r}{h} + 1.444\right)} \quad (19)$$

The above equations leads to the dimensions of  $L_1 = 4$  mm,  $W_1 = 2$  mm and  $W_2 = 8$  mm. The capacitance can be tuned and it causes fringing effect between patch and ground plane. This cutout discontinuity shifts the second resonant frequency 11 GHz and lowers the peaks to -31.5 dB. This microstrip discontinuity aids in improving the impedance bandwidth of the antenna 2.

The stub with length  $L_{stub} = 7.5$  mm and  $W_{stub} = 2$  mm is inserted as shown in Fig. 6 and it is the evolution of antenna 3

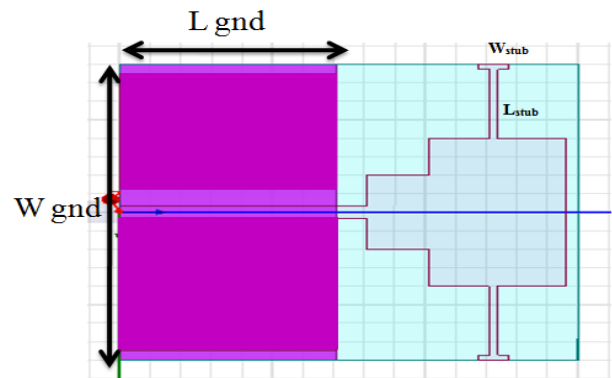


Fig. 6. Evolution of antenna 3 with insertion of stub (color online)

The evolution of antenna 3 shifts the first resonance to 3.2GHz thus improving the impedance bandwidth over the entire operating band. The return loss peak is lowered to -31 dB. The simulated results of the proposed UWB antenna are shown in Fig. 7.

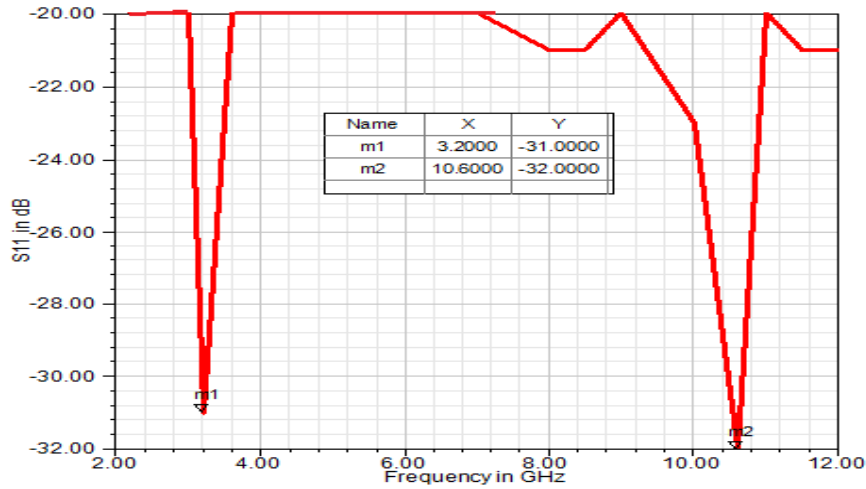


Fig. 7. Simulated Result of the proposed UWB antenna (color online)

This partial ground plane helps in maintaining flat impedance bandwidth over the operating band. The proposed antenna is tested with different ground plane which is listed in Table 1.

Table. 1. Dimensions of ground plane

$W_g$ (mm)	$L_g$ (mm)	Bandwidth
32	14.2	Below -10dB(3.1-10.6 GHz)
32	15.2	Below -10dB(5-10 GHz)
32	16.2	Below -10dB(5.9-8.2 GHz)
32	17.2	Above -10dB

From the above table it is clear that the ground with length 14.2 mm gives better results than the others.

### 3.2. Reconfigurable antenna

After designing a suitable UWB antenna, reconfigurable antenna is obtained with slots and switches in the ground plane [12]. This is the evolution of antenna 4 as shown in Fig. 8. The wideband characteristics can be switched to narrowband with the help of slots in the ground plane [13]. The switches vary the length of the slot. This helps to change the resonant frequencies.

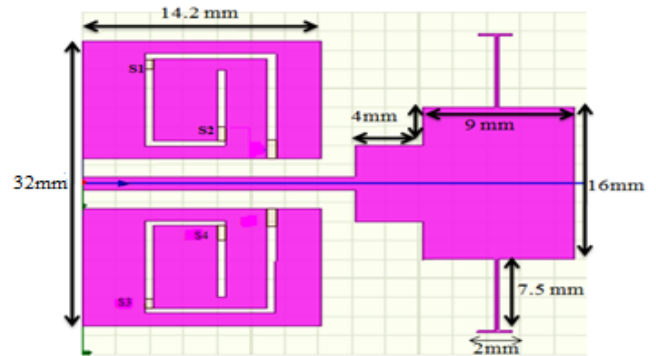


Fig. 8. Evolution of antenna 4 with slots and switches (color online)

The length and width of the slot [14] is designed using Eq. (20)

$$L_s = W_s = \frac{c}{6.2\sqrt{\epsilon_{\text{reff}}}} - \frac{3}{2}(L + \Delta L + S) \quad (20)$$

where slot thickness is given by Eq. (21)

$$S = \frac{\lambda_o}{60} \quad (21)$$

where  $\lambda_o$  is given by Eq. (22)

$$\lambda_o = \frac{c}{f_o} \quad (22)$$

$f_o$  is the resonant frequency  
 $L$  and  $\Delta L$  is defined by (4) and (5). When S1 and S2 are switched ON, S3 and S4 are switched OFF the resonant frequency is 6.0 GHz with return loss of -21 dB . When S3 and S4 are switched ON, S1 and S2 are switched OFF the resonant frequency is 4.9 GHz with return loss of -22dB.

When all the switches are in OFF condition the frequency obtained is 7.4GHz and 6.6 GHz. The narrow band is observed for the switching conditions S1 and S2 from 5.8 to 6.4 GHz and S3 and S4 from 7.2 to 7.6 GHz. The switching conditions are depicted in Table 2.

Table 2. Switches in different positions

Case	SW1	SW2	SW3	SW4	Resonance
1	ON	ON	OFF	OFF	6.0GHz
2	OFF	OFF	ON	ON	4.9GHz
3	OFF	OFF	OFF	OFF	7.4GHz,6.6GHz
4	ON	ON	ON	ON	UWB

The evolution of antenna 4 is explaining the reconfigurable concept by switching to narrow band [15]. When all the switches are ON it is UWB. It can be tuned to different frequencies for cognitive radio applications. The simulated results show good reconfigurable features as shown in Fig. 9.

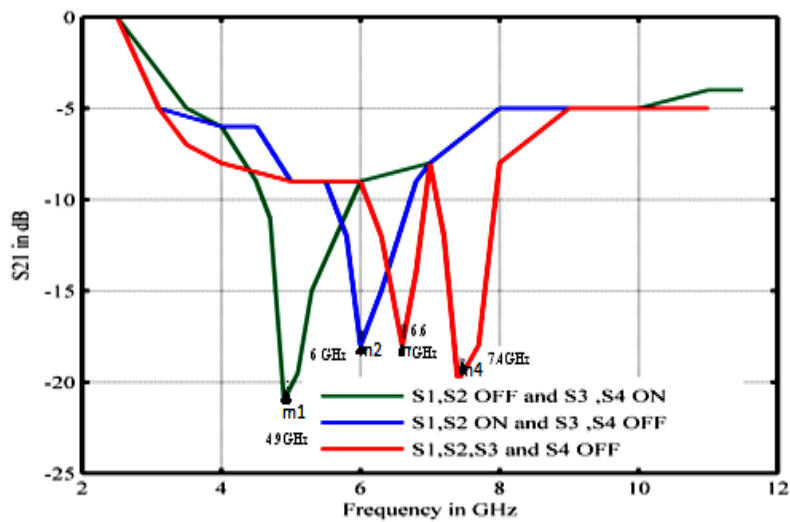


Fig. 9. Reconfigurability of the proposed antenna (color online)

### 3.3. The biasing circuit

The reconfigurable antennas make use of RF switch to alter the properties of antenna. This PIN diode RF switch is the ideal antenna switch for VHF and UHF .These PIN diodes which are special high frequency switching diodes with very low internal capacitance. The internal series resistance of a PIN diode can be remotely varied from 1 to 10.000  $\Omega$  by a DC control voltage. The parallel resistance is 470 $\Omega$  to 1 K $\Omega$ . The resistance of a PIN diode changes linearly in relation to the current flowing through it. The equivalent circuit of PIN diode in forward and reverse condition is shown in Fig. 10(a) and 10(b).

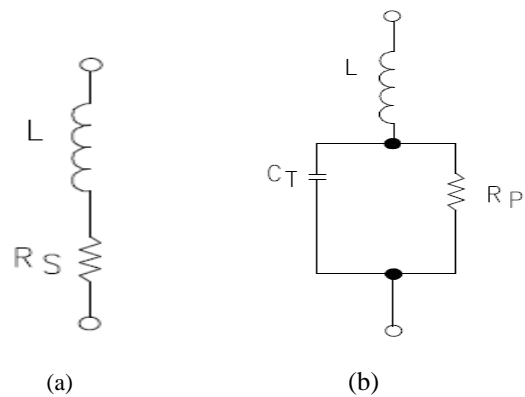


Fig. 10. (a) Forward bias equivalent circuit of PIN diode (b) Reverse bias equivalent circuit of PIN diode

The equivalent circuit for the forward biased PIN diode, Fig. 10(a), consists of a series combination of the series resistance ( $R_s$ ) and a small Inductance ( $L_s$ ). The PIN diode must be forward biased (Low Loss or ON State) so that the stored charge,  $Q_s$ , is much larger than the RF induced charge that is added or removed from the Intrinsic

region cyclically by the RF current as investigated in [16]. This relationship is shown by the inequality as in Eq. (23)

$$Q_s \gg \frac{I_{rf}}{2\pi f} \quad (23)$$

The Reverse Bias Equivalent Circuit as analyzed in [16] consists of the PIN diode Capacitance ( $C_T$ ), a shunt loss element ( $R_p$ ), and the parasitic Inductance ( $L_s$ ). A PIN diode, designed for high frequency operation is usually fabricated to have low capacitance because the reactance of the diode in the OFF condition must be large compared to the line impedance. The ratio of the PIN's area to thickness is adjusted to obtain the desired capacitance. The parametric values are chosen to be  $L=0.65\text{nH}$ ,  $R_S=3.2\Omega$ ,  $R_p=1\text{K}\Omega$ ,  $C_T=0.01\text{pF}$ .

The PIN diodes were modeled in HFSS using lumped RLC components.

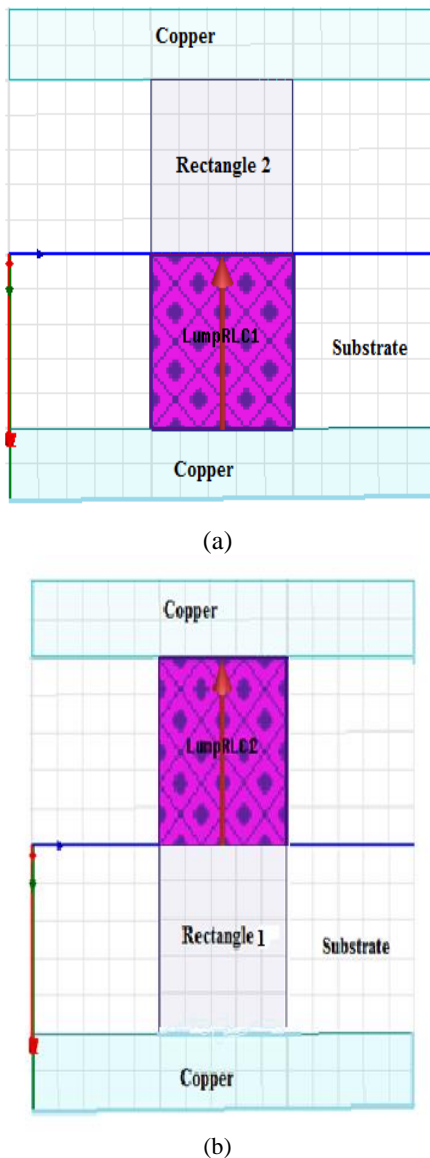


Fig. 11. Modeling of PIN diode (a) Assigning first lumped element (b) Assigning second lumped element (color online)

The two rectangular or square patches are drawn between the gap of the copper as shown in Fig. 11. These patches are modeled by clicking excitations as lumped RLC elements. The first rectangle is assigned an inductor and an arrow is assigned for its boundary excitation as in Fig. 11(a), the second rectangle is assigned as resistor and its value is  $R_S = 3.2 \Omega$  as shown in Fig. 11(b) for the ON state of the diode. The first rectangular element is not changed but the values of the second lumped elements are changed from  $R_S$  to  $R_p$  and also a parallel capacitance  $C_T$  is added for the OFF state. The PIN diode is connected between the copper traces. Two chokes can be used on both sides of the diode. They are connected via cable to provide DC bias voltage. A DC bias of 0.7V is applied for the ON state and the other part is connected to ground. This biasing is done because it offers very high impedance to RF signals to prevent it from flowing into DC bias lines. This reconfigurable switch is used for all prototype measurements.

#### 4. Results and discussion

Since the main interest of this work to create UWB and simultaneous reconfigurable resonance within the UWB, the impedance responses at these bands are important to be observed. Within the band of 5-6 GHz, the VSWR shows a slightly upward trend that might become problematic in the reconfiguration process. Therefore, to improve the matching further, the bottom radiating part is modified by truncating it which is viewed as microstrip discontinuity. Despite this truncation, the lower edge still has similar length, thus it does not degrade the antenna characteristics but rather improves impedance matching at the 5-6 GHz band. This modification allows the surface currents along the radiator's upper edges to be more concentrated and results in lower VSWR ( $< 2$ ) as shown in Fig. 12.

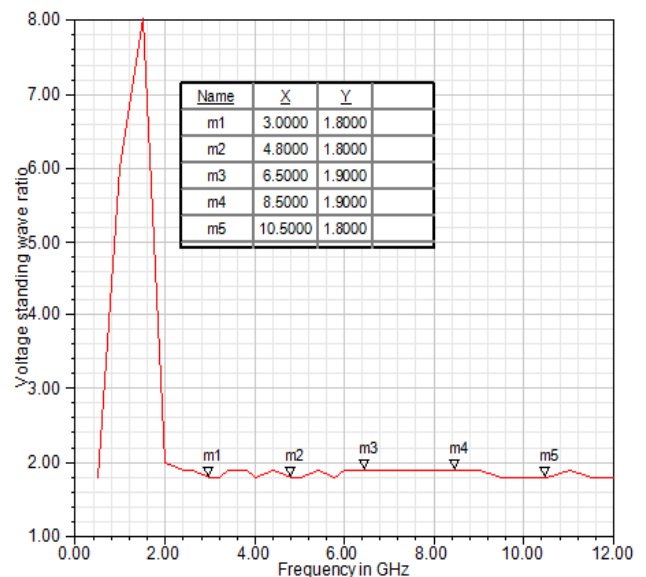


Fig. 12. Simulated VSWR against frequency (color online)

It is obvious from the Fig. 12, the values of VSWR is almost less than 2 over the simulated UWB. The simulated gain plot versus frequency is shown in Fig. 13. It is

observed that the gain of the proposed antenna lies between 5 and 6.5 dBi throughout the operating band.

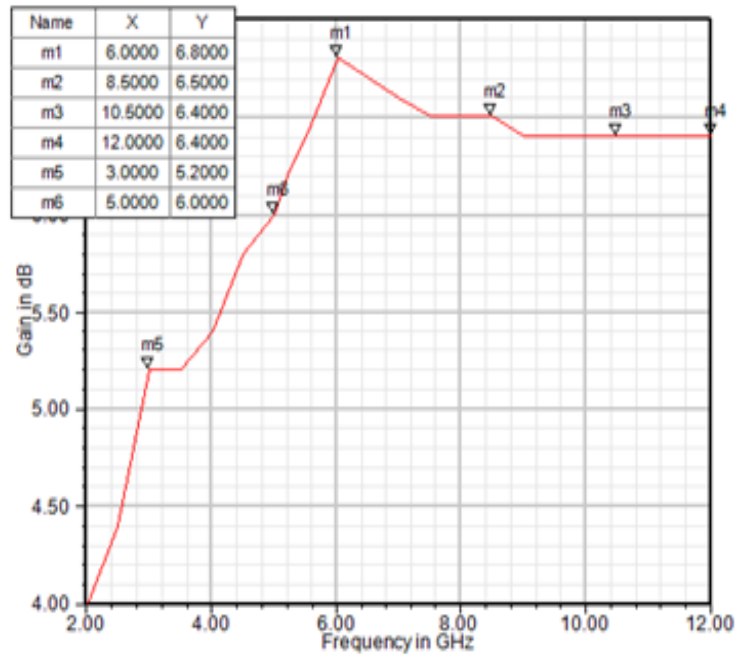


Fig. 13. Simulated result of gain versus frequency (color online)

Fig. 14(a) and (b) illustrates the radiation patterns of the antenna in terms of H-plane and E-plane respectively. Based on figure, for E-plane it could be observed that the antenna displays an eight shaped pattern with its concentration focusing on the sides of the patch antenna. As of the H-plane, the patterns exhibit omnidirectional patterns throughout the simulated frequency which is

expected. The proposed antenna preserves stable radiation in both planes at almost all the frequencies. The proposed antenna shows ultra wideband features in terms of return loss and impedance BW in the simulated result as shown in Fig. 7. The proposed antenna gives better result when ground length is 14.2 mm. The simulated results show good reconfigurable features as shown in Fig. 9.

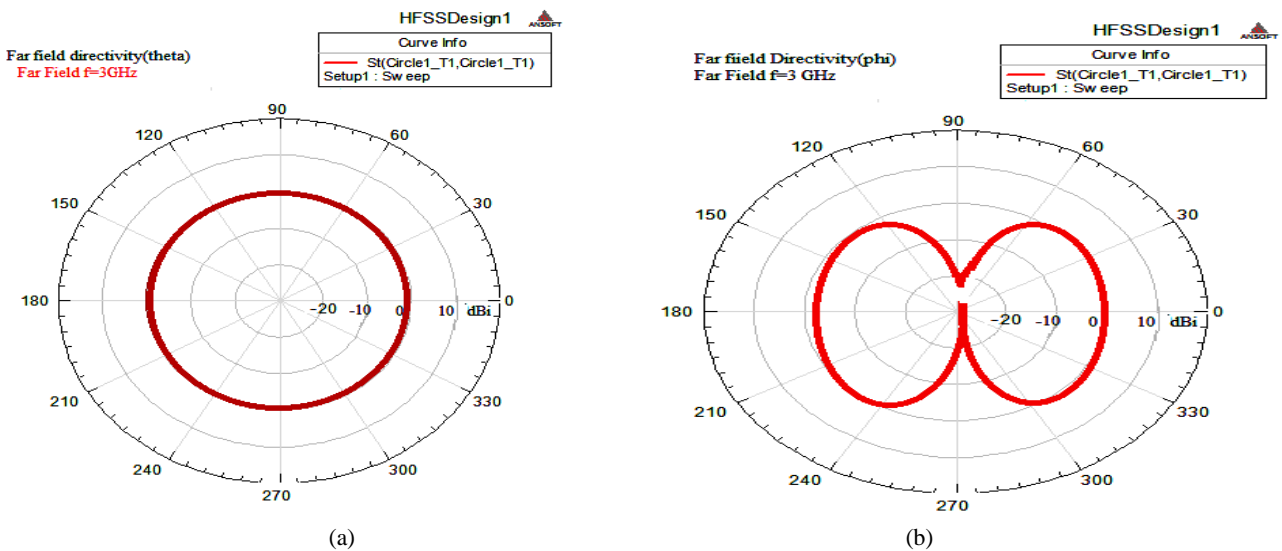


Fig. 14. Simulated (a) H-field (b) E-field radiation patterns for the proposed antenna at 3GHz (color online)

**4.1. Experimental results**

The fabricated prototype of frequency reconfigurable antenna with pin diode is shown in Fig. 15.



Fig. 15. Fabricated prototype of the proposed antenna

Fig. 16 illustrates the pin diode with proper dc biasing in a fabricated prototype. The dc bias lines are properly RF choked using inductors and resistances.

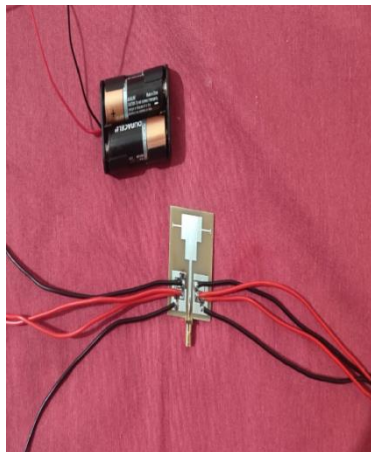
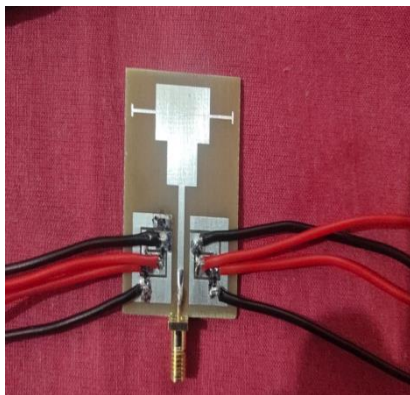


Fig. 16. Fabricated prototype of the biasing structure (color online)

When all the switches are ON the antenna is working in ultra wideband mode with a return loss of -31dB. The measured results show good agreement with the simulated results as in Fig. 17.

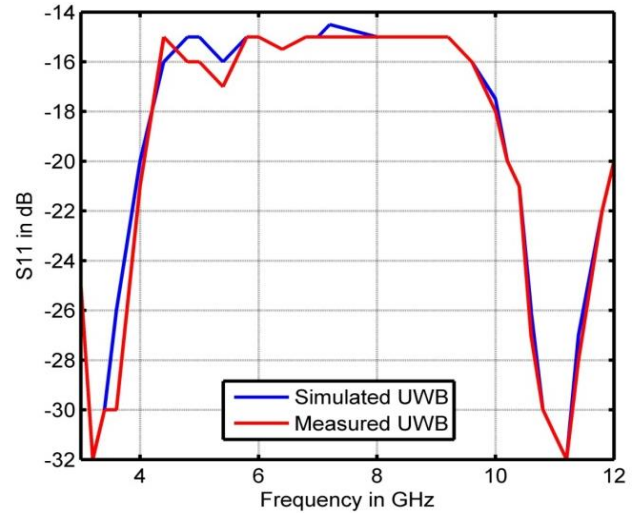


Fig. 17. Simulated and Measured return loss with switches ON (color online)

The simulated and measured return loss when all the switches are OFF is shown in Fig. 18. The designed antenna operates at the resonant frequency of 6.6GHz and 7.4GHz with a return loss of about -20dB. The measured results are in good agreement with the simulated results. In the experimental setup the PIN diodes with low capacitance which can operate upto 8GHz is selected. When the diode is forward biased it performs as series resistor. The reverse bias works as a series capacitor. The feeding path of the fabricated antenna is completely isolated from the DC path. The switching action is performed due to the presence of capacitor and RF choke.

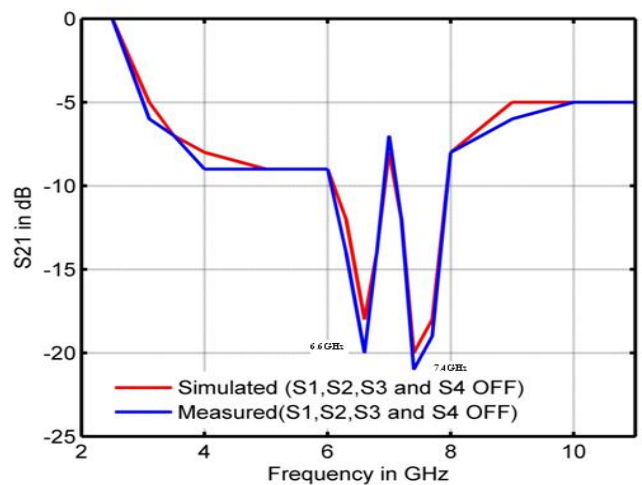
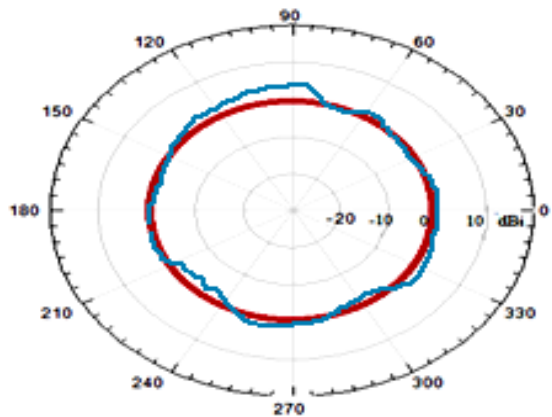
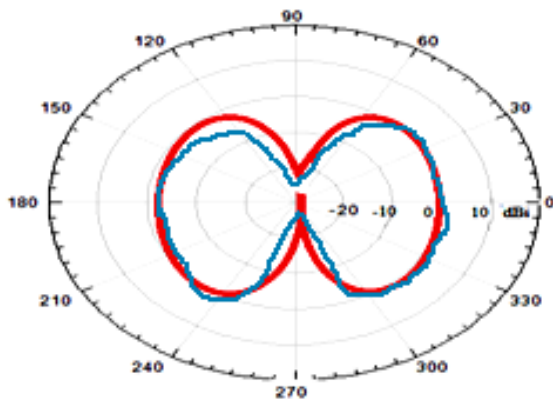


Fig. 18. Simulated and Measured return loss with switches OFF (color online)



(a)



(b)

Fig. 19. (a) Simulated (solid red line) and Measured (solid blue line) H plane radiation pattern when the antenna is configured at 3 GHz. (b) Simulated (solid red line) and Measured (solid blue line) E plane radiation pattern when the antenna is configured at 3 GHz (color online)

The simulated and measured radiation pattern when the antenna is configured at 3 GHz is shown in Fig. 19. It is observed that H plane pattern is omnidirectional and is similar to what is obtained in simulation. The simulated and measured E plane pattern is almost same and E shape like traditional monopole. There are some minor distortions in the measured curve. These ripples are caused by feed connector and coaxial cable used in the measurement.

#### 4.2. Comparison with the recent work in literature

The antenna is comparable with other recent structure similar to the proposed antenna in terms of the size, entire UWB, number of reconfigurable operation modes.

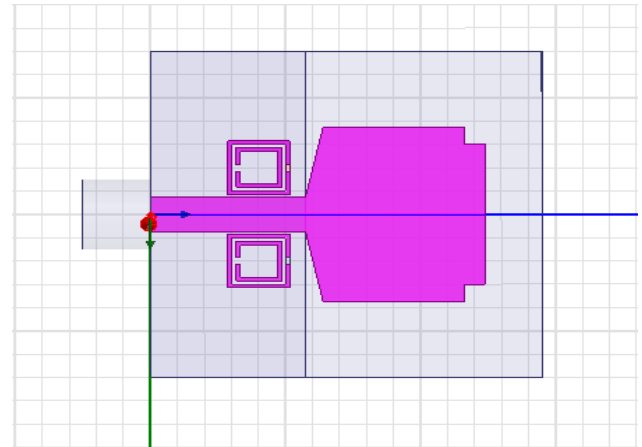


Fig. 20. Structure of the existing reconfigurable antenna (color online)

The structure of existing structure is shown in Fig. 20. The size of the existing is 1600 Sq.mm, whereas the proposed antenna is 900 Sq.mm. The antenna covers the ultra wide band from 4.2 GHz to 10 GHz as in Fig. 21. The proposed antenna in comparison has wider bandwidth from 3.1GHz to 10.6GHz. The proposed can switch to four reconfigurable modes in comparison to existing antenna which has one reconfigurable mode.

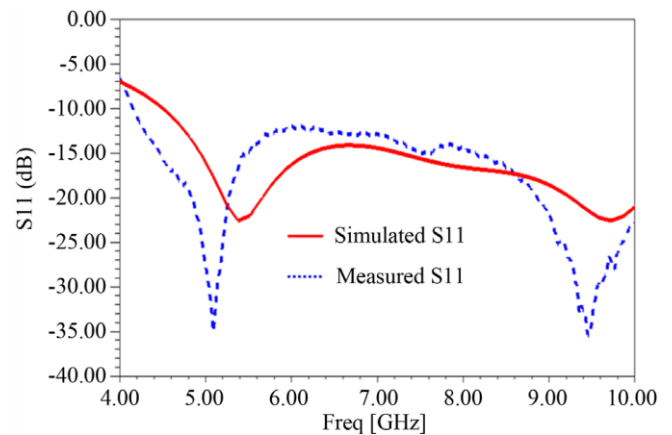


Fig. 21. UWB response of the existing antenna (color online)

#### 5. Conclusion

In this work, modeling the microstrip structure for cognitive radio application has been proposed. A frequency reconfigurable antenna with PIN diode is designed and fabricated. The measured results are in good agreement with the simulated ones. The proposed antenna maintains impedance bandwidth over the operating band from 3.1GHz to 10.6GHz. Moreover, this antenna has the unique feature of reversibility between the narrow band modes and the normal UWB operations. These characteristics enable the proposed structure to mark its significance in cognitive radio applications. This work

modeled consistently provides an efficient way to realize multiple frequency bands in a limited space.

## References

- [1] L. Huang, P. Russer, *IEEE Transactions on Microwave Theory and Techniques* **56**(12), 2789 (2008).
- [2] A. Iqbal, A. Smida, N. K. Mallat, R. Ghayoula, I. Elfergani, J. Rodriguez, S. Kim, *Electronics* **8**(4), 407 (2019).
- [3] K. Hakim, S. K. Jayaweera, G. El-Howayek, C. Mosquera, *IEEE Transactions on Wireless Communications* **9**(9), 2956 (2010).
- [4] S. Yang, C. Zhang, H. K. Pan, A. E. Fathy, V. K. Nair, *IEEE Microwave Magazine* **10**(1), 66 (2009).
- [5] G. Dubost, S. Zisler, *Antennes à Large Bande: théorie et applications* 128 (1976).
- [6] N. G. Alexopoulos, D. R. Jackson, *IEEE Trans. Antennas and Propagation* **32**(8), 807 (1984).
- [7] Constantine A. Balanis, *Antenna theory: analysis and design*, John Wiley & Sons, Inc., Publication (2005).
- [8] K. G. Thomas, M. Sreenivasan, *IEEE Transactions on Antennas and Propagation* **58**(1), 27 (2010).
- [9] I. J. Bahl, *Lumped elements for RF and microwave circuits*, Artechhouse, (2003).
- [10] I. Pele, Y Mahe, A. Chousseaud, S. Toutain, P. Y. Garel, *Antennas and Propagation Society International Symposium 1.IEEE*, 783 (2004).
- [11] T. C. Edwards, *Foundations for microstrip circuit design*, John Wiley and Sons Canada Limited, (1992).
- [12] Ansys, Inc., Ansoft HFSS, ver. 15.0 [Online]. Available:www.ansoft.com.
- [13] L. Liu, S. W. Cheung, T. I. Yuk, *Proc. Prog Electromagn. Res. Symp. (PIERS)*, Suzhou, China, 1420 (2011).
- [14] O. Kumar, S. K. Soni, *MATEC Web of Conferences, EDP Sciences* **57**, 01020 (2016).
- [15] H. A. Majid, M. K. A. Rahim, M. R. Hamid, M. F. Ismail, F. Malek, *Journal of Electromagnetic Waves and Applications* **26**(11-12), 1460 (2012).
- [16] W. E. Doherty, R. D. Joos, *The PIN diode circuit designers Handbook*, Microsemi Corporation **1**, 1-137 (1998).

---

\*Corresponding author: talkto2006@gmail.com